

## Electronic Supplementary Information

### Utilization of solar energy for continuous bioethanol production for energy applications

Betina Tabah<sup>[a]</sup>, Indra Neel Pulidindi<sup>[a]</sup>, Venkateswara Rao Chitturi<sup>[c]</sup>, Leela Mohana  
Reddy Arava<sup>[c]</sup>, and Aharon Gedanken\*<sup>[a, b]</sup>

<sup>[a]</sup>Department of Chemistry, Bar-Ilan University, Ramat-Gan 52900, Israel

<sup>[b]</sup>Department of Materials Science and Engineering, National Cheng Kung University, Tainan  
70101, Taiwan

<sup>[c]</sup>Department of Mechanical Engineering, Wayne State University, Detroit, MI 48202, USA

*\*Corresponding author:*

*Tel: +972-3-5318315; Fax: +972-3-7384053; e-mail: gedanken@mail.biu.ac.il*

### The design and the fabrication of the solar reactor:

The aluminum blocks used for fabricating the bottom (325 x 275 x 120 mm, length, width, and height, respectively) and top (325 x 275 x 6.3 mm) portions of the reactor were purchased from Jack Eini International (metals) Trade Ltd., Israel. The reactor was fabricated in the mechanical workshop of Bar-Ilan University by Mr. Menachem Schneeberg. As depicted in Fig. S1, the ethanol collection chamber (second chamber) was well separated from the fermentation chamber (first chamber) by an aluminum wall. The inlet of the reactor was connected to the glucose solution reservoir and the ethanol outlet valve was opened for collecting the product (ethanol) at regular time intervals. The analyte can also be collected from the yeast bed (first chamber) via fermentation broth outlet without opening the reactor lid.

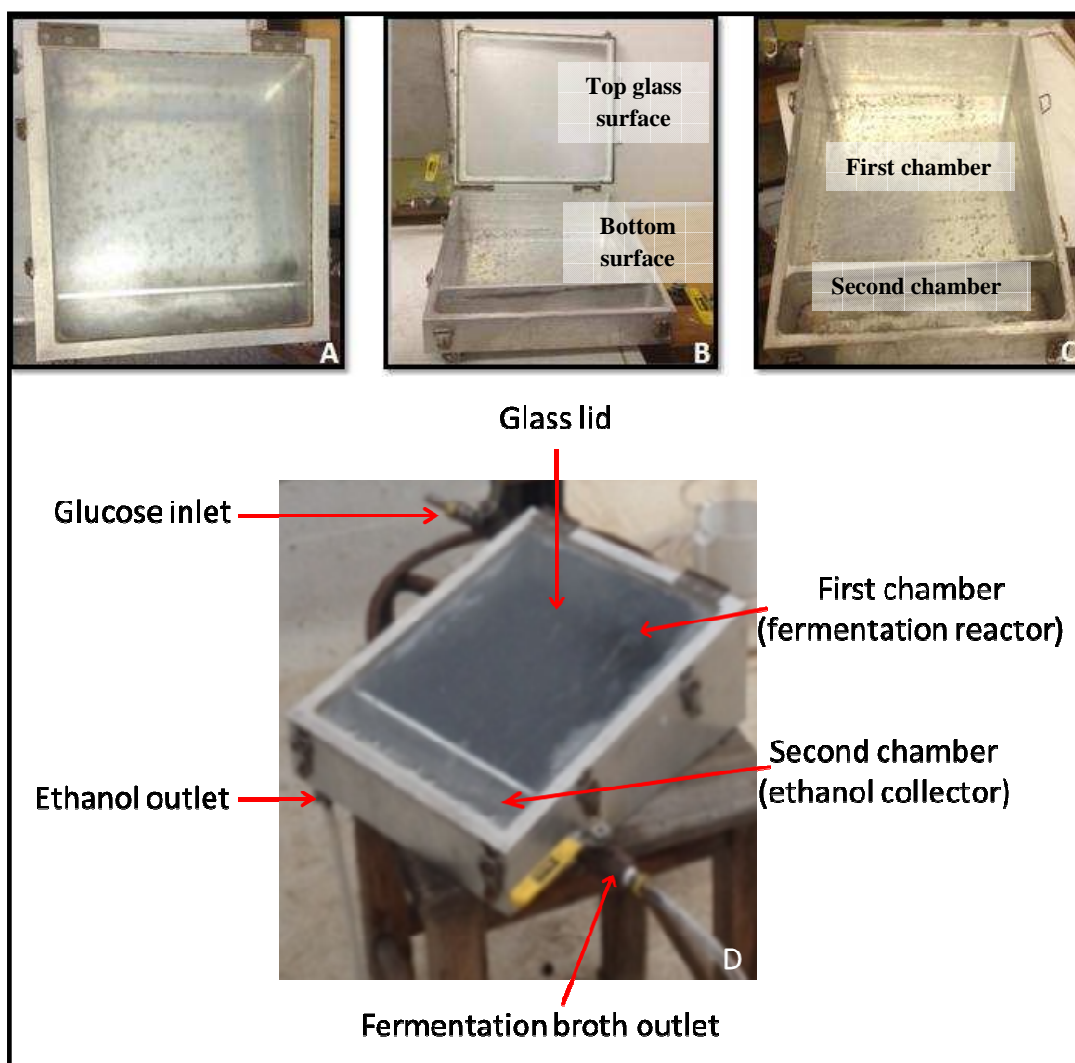


**Fig. S1** The design of the solar reactor: (A) closed reactor (B) open reactor (C) the base of the reactor with two chambers, and (D) all the components of the reactor

### Theoretical yield of ethanol from glucose fermentation:

Theoretically, each mole of glucose (consumed by yeast) results in two moles of ethanol as a metabolite (Eq. S1). Thus, a maximum of 0.51 g ethanol could be produced from 1.0 g glucose, the rest being converted to CO<sub>2</sub> (0.49 g).

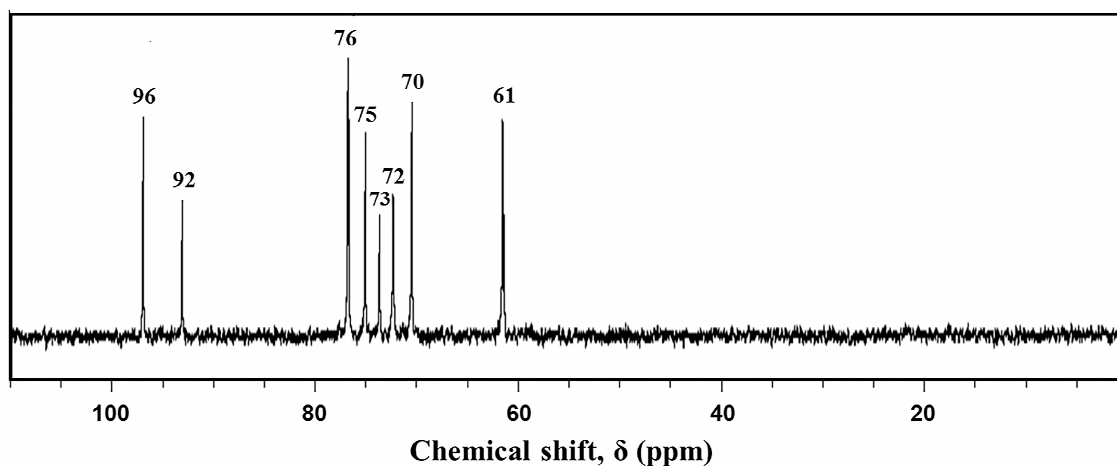
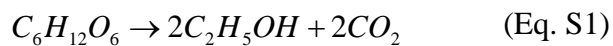


Fig. S2 <sup>13</sup>C NMR spectrum of authentic glucose

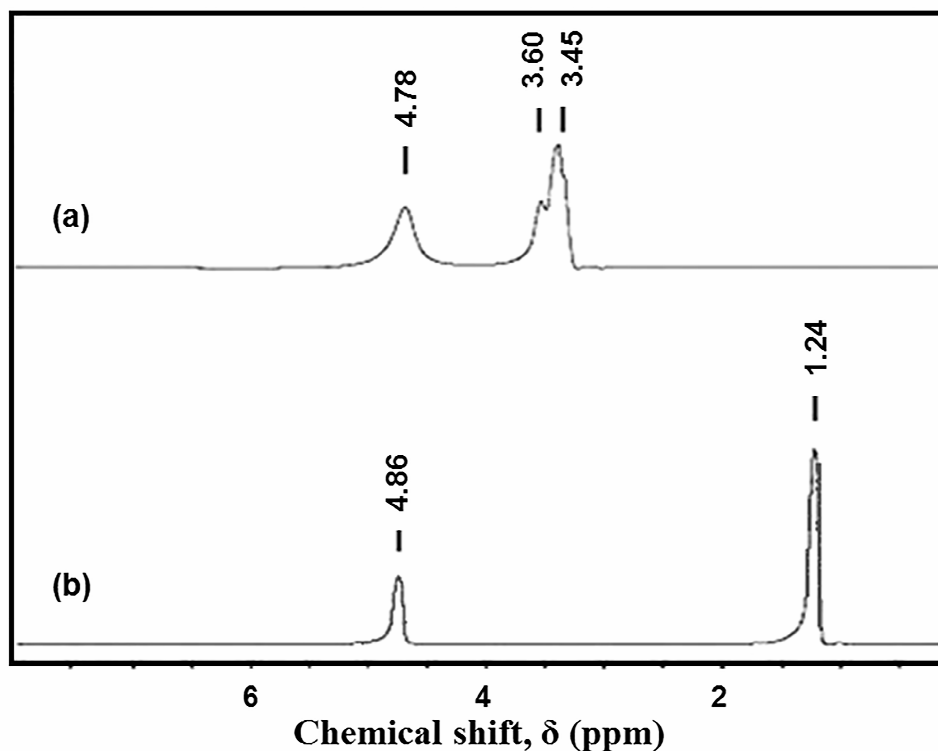
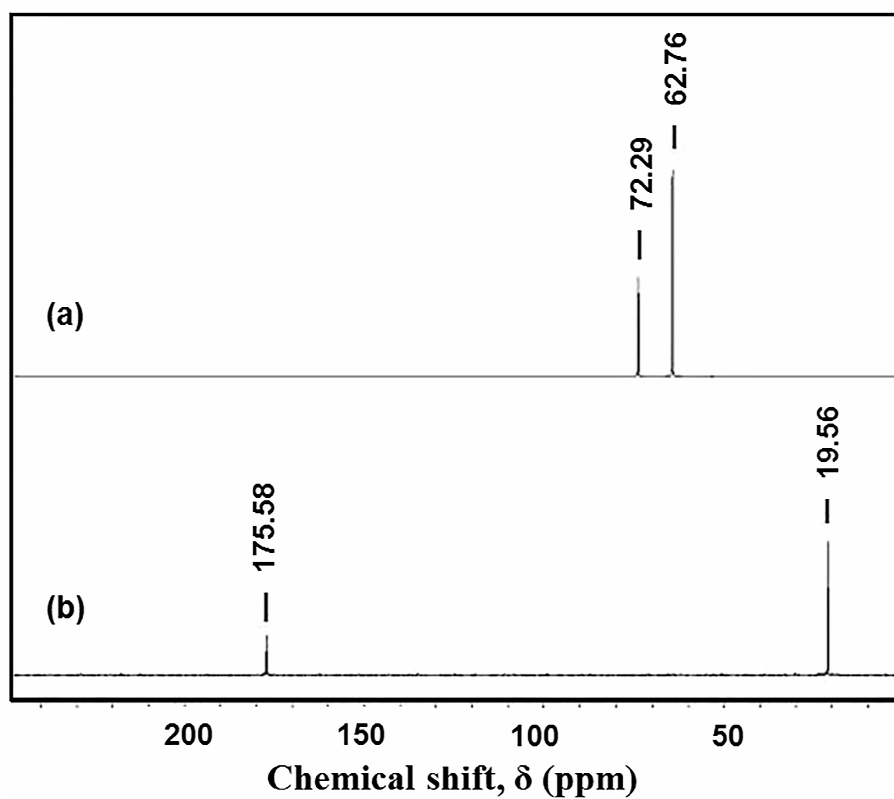


Fig. S3 <sup>1</sup>H NMR spectra of authentic (a) glycerol and (b) acetic acid (the peak at ~ 4.80 ppm corresponds to the solvent)



**Fig. S4** <sup>13</sup>C NMR spectra of authentic (a) glycerol and (b) acetic acid

**Table S1** Comparison of ethanol concentrations (fermentation product) deduced from GC and <sup>1</sup>H NMR analyses from 10 wt.% glucose solution

Analyte	Ethanol concentration (M)	
	GC analysis	<sup>1</sup> H NMR analysis
5 <sup>th</sup> day	0.86	1.01
10 <sup>th</sup> day	1.14	1.10
15 <sup>th</sup> day	1.26	1.12
20 <sup>th</sup> day	1.08	1.13
25 <sup>th</sup> day	1.04	1.12

**Table S2** Comparison of ethanol concentrations (fermentation product) deduced from GC and  $^1\text{H}$  NMR analyses from 20 wt.% glucose solution

Analyte	Ethanol concentration (M)	
	GC analysis	$^1\text{H}$ NMR analysis
5 <sup>th</sup> day	1.57	1.72
10 <sup>th</sup> day	1.55	1.75
15 <sup>th</sup> day	1.68	1.74
20 <sup>th</sup> day	1.80	2.04
25 <sup>th</sup> day	1.85	2.10

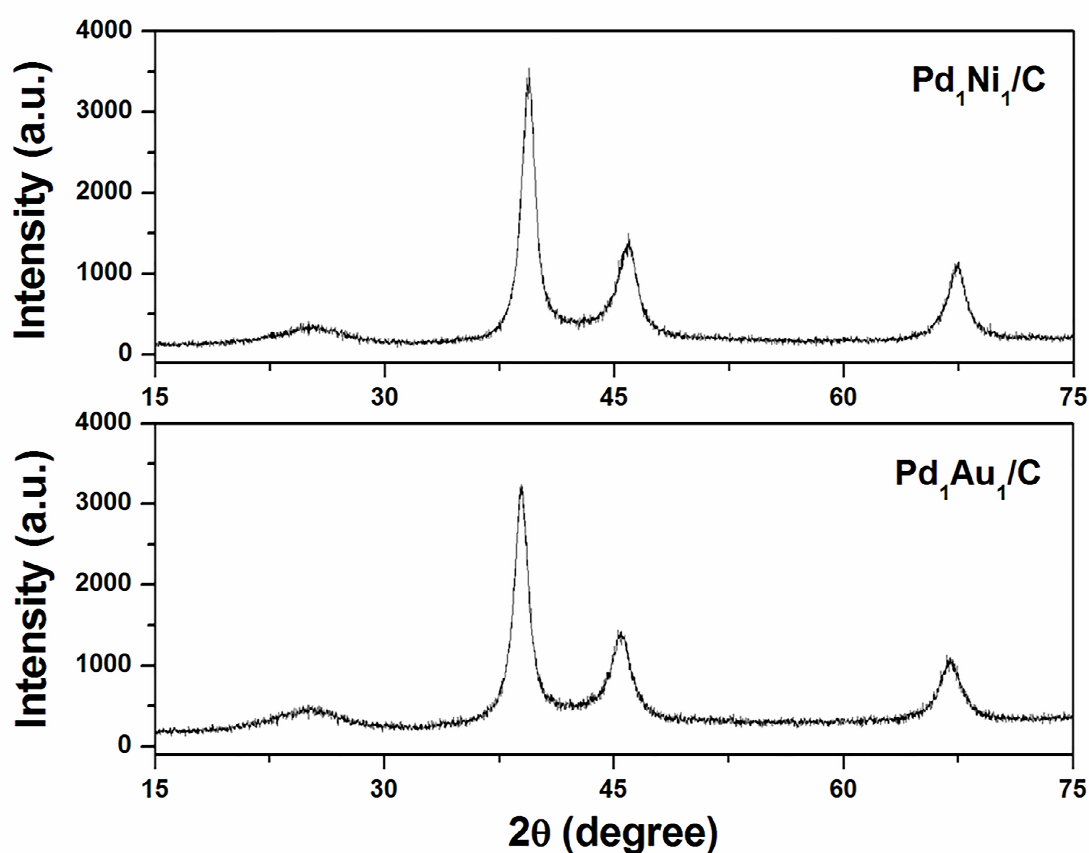


**Fig. S5** Powder XRD patterns recorded for  $\text{Pd}_1\text{Ni}_1/\text{C}$  and  $\text{Pd}_1\text{Au}_1/\text{C}$  catalysts

Powder XRD measurements were performed to evaluate the microstructure of the catalysts. The XRD pattern is shown in Fig. S5. The position of the diffraction peaks of the different crystallographic planes indicates the existence of face-centered cubic (FCC) crystalline structure. A weak shift of the diffraction peak position corresponding to the (111) peak of palladium is detected in both cases which is an indication of Pd-M alloy formation. ICP-MS analysis revealed the bulk atomic composition of Pd/M as 53/47 and 51/49 for  $\text{Pd}_1\text{Ni}_1/\text{C}$  and  $\text{Pd}_1\text{Au}_1/\text{C}$  catalysts, respectively.

**Table S3.** AA-DEFC performances reported in the literature and the present work

Fuel	Oxidant	Anode	Cathode	Membrane	Temp. (K)	Power density (mW/cm <sup>2</sup> )	Ref.
3 M Ethanol + 5 M NaOH	4 M H <sub>2</sub> O <sub>2</sub> + 1 M H <sub>2</sub> SO <sub>4</sub>	PdNi/C	Pt/C	NaOH-treated Nafion211	333	360	1
3 M Ethanol + 5 M NaOH	4 M H <sub>2</sub> O <sub>2</sub> + 1 M H <sub>2</sub> SO <sub>4</sub>	PdNi/C	Pt/C	NaOH-treated Nafion117	333	240	2
3 M Ethanol + 5 M NaOH	4 M H <sub>2</sub> O <sub>2</sub> + 1 M H <sub>2</sub> SO <sub>4</sub>	PdNi/C	Au@Ni-Cr foam	NaOH-treated Nafion211	333	200	3
3 M Ethanol + 5 M KOH	4 M H <sub>2</sub> O <sub>2</sub>	PdNi/C	Acta Hypermec, K14	Anion exchange membrane, A201	333	130	4
2 M Bio-ethanol + 5 M KOH	4 M H <sub>2</sub> O <sub>2</sub> + 1 M H <sub>2</sub> SO <sub>4</sub>	PdNi/C	PdAu/C	NaOH-treated Nafion211	303 and 333	330 (at 303 K) 410 (at 333 K)	This work

## References

- 1 L. An and T.S. Zhao, *Int. J. Hydrogen Energy*, 2011, **36**, 9994-9999.
- 2 L. An, T.S. Zhao, R. Chen and Q.X. Wu, *J. Power Sources*, 2011, **196**, 6219-6222.
- 3 L. An, T.S. Zhao and J.B. Xu, *Int. J. Hydrogen Energy*, 2011, **36**, 13089-13095.
- 4 L. An, T.S. Zhao, L. Zeng and X.H. Yan, *Int. J. Hydrogen Energy*, 2014, **39**, 2320-2324.